ANL/ET/CP--89687 CONF-960706--16

EFFECTS OF LWR COOLANT ENVIRONMENTS ON FATIGUE S–N CURVES FOR CARBON AND LOW–ALLOY STEELS*

Omesh K. Chopra and William J. Shack
Energy Technology Division
Argonne National Laboratory
Argonne, Illinois, 60439, USA

DISCLAIMER

March 1996

For presentation at 1996 Pressure Vessel and Piping Conference, Montreal, Quebec, Canada, July 21–27, 1996

*Work supported by the Office of Nuclear Regulatory Research of the U.S. Nuclear Regulatory Commission, under FIN Number W6610; Program Manager: Dr. M. McNeil.

EFFECTS OF LWR COOLANT ENVIRONMENTS ON FATIGUE S–N CURVES FOR CARBON AND LOW–ALLOY STEELS

Omesh K. Chopra and William J. Shack
Energy Technology Division
Argonne National Laboratory
Argonne, Illinois 60439

ABSTRACT

The ASME Boiler and Pressure Vessel Code provides rules for the construction of nuclear power plant components. Figure I–90 of Appendix I to Section III of the Code specifies fatigue design curves for structural materials. However, the effects of light water reactor (LWR) coolant environments are not explicitly addressed by the Code design curves. Recent test data indicate significant decreases in fatigue lives of carbon and low–alloy steels in LWR environments when five conditions are satisfied simultaneously: applied strain range, temperature, dissolved oxygen in the water, and S content of the steel are above minimum threshold levels, and loading strain rate is below a threshold value. Only moderate decrease in fatigue life is observed when any one of these conditions is not satisfied. This paper presents several methods that have been proposed for evaluating the effects of LWR coolant environments on fatigue S–N curves for carbon and low–alloy steels. Estimations of fatigue lives under actual loading histories are discussed.

INTRODUCTION

The ASME Boiler and Pressure Vessel Code Section III, which contains rules for the construction of Class 1 components for nuclear power plants, recognizes fatigue as a possible mode of failure in pressure vessel steels and piping materials. Cyclic loadings on a structural component occur as a system moves from one load set (e.g., pressure, temperature, moment, and force loading) to any other load set. For each pair of load sets, an individual fatigue usage factor is determined by the ratio of the number of cycles anticipated during the lifetime of the component to the allowable cycles. Figure I–90 of Appendix I to Section III of the Code specifies fatigue design curves that define the allowable number of cycles for a given alternating stress amplitude. The cumulative usage factor (CUF) is the sum of the individual usage factors. The ASME Code Section III requires that the CUF at each location must not exceed a value of 1.

The current Code fatigue design curves are based on strain–controlled tests of small polished specimens at room temperature (RT) in air. The fatigue design curves were obtained by decreasing the best–fit curves to the experimental data by a factor of 2 on stress or 20 on cycles, whichever was more conservative, at each point on the best–fit curve. These factors are not safety margins but rather conversion factors that must be applied to the experimental data to obtain reasonable estimates of the lives of actual reactor components. For example, the factor of 20 on cycles is the product of three subfactors: 2 for scatter of data (minimum to mean), 2.5 for size effects, and 4 for surface finish, etc. The effect of LWR coolant environments on fatigue resistance of the material is not explicitly addressed in the Code design fatigue curves.

The existing fatigue strain vs. life (S–N) data [1–4] illustrate potentially significant effects of LWR coolant environments on the fatigue resistance of carbon steels (CSs) and low–alloy steels (LASs). Environmental effects on fatigue life are significant when five conditions are satisfied simultaneously, i.e., when applied strain range, service temperature, dissolved oxygen (DO) in the water, and S content of the steel are above minimum threshold levels, and loading strain rate is below a threshold value. Environmental effects on fatigue life are modest when any one of the threshold conditions is not satisfied. Interim fatigue design curves have been developed that account for temperature, DO content in water, S level in steel, and strain rate [5]. Statistical models have also been developed for estimating the effects of various material and loading conditions on fatigue lives of materials used in the construction of nuclear power plant components [6]. The Pressure Vessel Research Council (PVRC) has also been compiling and evaluating fatigue S–N data related to the effects of LWR coolant environments on the fatigue life of pressure boundary materials [7].

This paper presents several methods that have been proposed for evaluating the effects of LWR coolant environments on fatigue S–

N curves for carbon and low–alloy steels. Estimations of fatigue lives under actual loading histories are discussed.

FATIGUE LIFE CORRECTION FACTOR

The analytical approach proposed by the Environmental Fatigue Data (EFD) Committee of the Thermal and Nuclear Power Engineering Society (TENPES) of Japan is based on the correlations described by Higuchi and Iida [8] and Higuchi et al. [9] and assumes that life in the environment N_{water} is related to life in air N_{air} at room temperature through a power–law dependence on strain rate. The fatigue life of a test specimen is defined as the number of cycles for the tensile stress to drop 25% from its peak value, which for test specimens with a 6– or 9–mm diameter corresponds to a ≈2.5– or ≈3.5–mm–deep crack, respectively. Thus, fatigue life represents the number of cycles required to initiate a crack approximately 3 mm deep. The EFD approach considers a fatigue life correction factor F_{en} to incorporate the effect of coolant environment on fatigue lives of CSs and LASs. To incorporate environmental effects into the ASME Code fatigue evaluation, a fatigue usage for a specific load pair based on the current Code fatigue design curve is multiplied by the correction factor. In air, the fatigue life N_{air} of CSs is expressed as

$$N_{air} = \left[\frac{(\varepsilon_a - 0.108)}{23.1}\right]^{-2.119} \tag{1a}$$

and of LASs

$$N_{air} = \left[\frac{(\varepsilon_a - 0.140)}{41.9}\right]^{-1.761}, \tag{1b}$$

where ε_a is the applied strain amplitude (%). The correction factor F_{en}, defined as the ratio of fatigue life in air to that in water, is expressed as

$$F_{en} = \frac{N_{air}}{N_{water}} = (\dot{\varepsilon})^{-P}, \tag{2}$$

where $\dot{\varepsilon}$ is the strain rate (%/s) during the tensile loading cycle. Only the tensile loading cycle is considered to be important for environmental effects on fatigue life. Recent fatigue data indicate that compressive loading cycle also decreases fatigue life, although the decrease in life is relatively small [1,3,9]. The exponent P is a function of temperature (T) and DO level given by

$$P = 0.1 + M(DO)\cdot N(T) \tag{3}$$

where for both CSs and LASs

$$M(DO) = \begin{cases} 0 & DO \le 0.1 \text{ ppm} \\ (DO - 0.1)/0.1 & 0.1 < DO < 0.2 \text{ ppm} \\ 1 & DO \ge 0.2, \end{cases} \tag{4a}$$

for CSs

$$N(T) = \begin{cases} 0.2\,T/100 & T \le 100°C \\ 0.2 & 100 < T < 200°C \\ 0.2 + 0.4\,(T - 200)/100 & T \ge 200°C, \end{cases} \tag{4b}$$

and for LASs

$$N(T) = \begin{cases} 0.175\,T/100 & T \le 100°C \\ 0.175 & 100 < T < 200°C \\ 0.175 + 0.075\,(T - 200)/100 & T \ge 200°C. \end{cases} \tag{4c}$$

The experimental values of fatigue life of CSs and LASs in water and those predicted from Eqs. 1–4 are plotted in Fig. 1. The current fatigue S–N data in water consist of ≈600 tests, equally divided between carbon and low–alloy steels, on 25 heats of steels tested at 25–320°C, DO levels of 0.01–8 ppm, and strain rates in the range of 0.0004–0.4%/s. Not all of these tests were used in developing the correlations. Higuchi and Iida [8] also defined a fatigue strength correction factor K_{en} expressed as

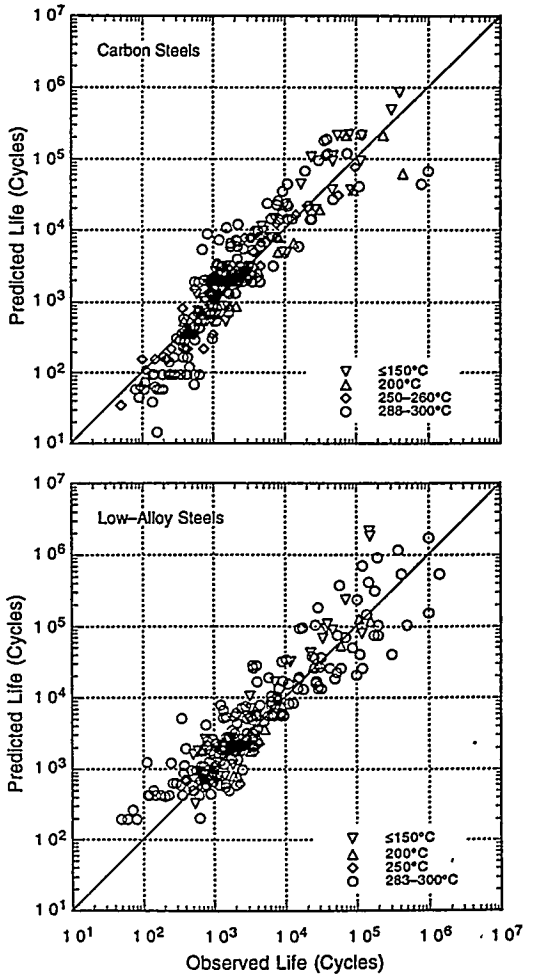

Figure 1. Fatigue lives of carbon and low–alloy steels estimated from correlations of Higuchi and Iida and determined experimentally in water

$$K_{en} = 1 + \left(\dot{\varepsilon}^{PB} - 1\right)\left(1 - \frac{C}{\varepsilon_a}\right), \quad (5)$$

where the values of the constant B are –0.472 and –0.568 (i.e., inverse of the exponent in Eq. 1) and of the constant C are 0.108 and 0.140, respectively, for CSs and LASs. The fatigue strength correction factor K_{en} is applied to the alternating stress amplitude S_a for a specific load pair, before the allowable fatigue cycles are determined from the fatigue design curves.

INTERIM FATIGUE DESIGN CURVE

The interim fatigue design curves are based on a modified version of Higuchi and Iida's correlations. The interim curves consider an effect of temperature on fatigue life even in air that is relatively independent of strain rate. Also, the parameters M(DO) and N(T) of Eq. 4 are defined for high– or low–S steels rather for carbon or low–alloy steels. In air, the fatigue life N_{air} of both CSs and LASs is expressed as

$$N_{air} = \left(\frac{\varepsilon_a}{0.6}\right)^{-7.692} + \left(\frac{\varepsilon_a}{25.5}\right)^{-2.132}, \quad (6)$$

where ε_a is the applied strain amplitude (%). The fatigue life in water is expressed as

$$N_{water} = N_{air}\Phi(T)\left(\dot{\varepsilon}\right)^{P}, \quad (7)$$

where

$$\Phi(T) = 0.6e^{148.5/(T+273)}, \quad (8)$$

for high–S steels (S ≥ 0.008 wt.%)

$$P = 0.04 + M(DO)\cdot N(T), \quad (9)$$

$$M(DO) = \begin{cases} 0 & DO \le 0.1 \text{ ppm} \\ (DO - 0.1)/0.1 & 0.1 < DO < 0.2 \text{ ppm} \\ 1 + 0.04\,(DO - 0.2) & DO \ge 0.2, \end{cases} \quad (10a)$$

$$N(T) = \begin{cases} 0.26\,T/100 & T \le 100°C \\ 0.26 & 100 < T < 200°C \\ 0.26 + 0.23\,(T - 200)/100 & T \ge 200°C, \end{cases} \quad (10b)$$

and for low–S steels (S < 0.008 wt.%)

$$P = 0.1 + M(DO)\cdot N(T), \quad (11)$$

$$M(DO) = \begin{cases} 0 & DO \le 0.1 \text{ ppm} \\ (DO - 0.1)/0.1 & 0.1 < DO < 0.2 \text{ ppm} \\ 1 & DO \ge 0.2, \end{cases} \quad (12a)$$

$$N(T) = \begin{cases} 0.175\,T/100 & T \le 100°C \\ 0.175 & 100 < T < 200°C \\ 0.175 + 0.075\,(T - 200)/100 & T \ge 200°C. \end{cases} \quad (12b)$$

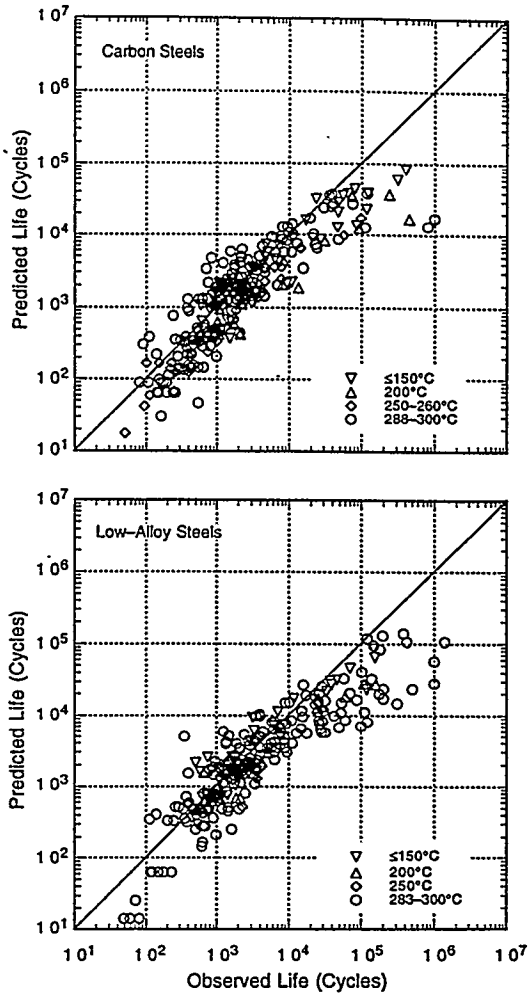

Figure 2. Fatigue lives of carbon and low–alloy steels estimated from correlations used in developing the interim design curves and determined experimentally in water

The temperature T is expressed in °C and strain rate $\dot{\varepsilon}$ in %/s. Strain rate during the tensile loading cycle is considered to be important for environmental effects on fatigue life. Equation 7 can be used to define a fatigue correction factor F_{en}. The experimental values of fatigue life of CSs and LASs in water and those estimated from Eqs. 6–12 are plotted in Fig. 2.

STATISTICAL MODEL

The fatigue life of CSs and LASs in air and LWR environments can be estimated from statistical models [6]. In air, the fatigue life N_{air} of CSs is expressed as

$$\ln(N_{air}) = 6.570 - 0.00133\,T - 1.871\,\ln(\varepsilon_a - 0.11) \quad (13a)$$

and that of LASs as

$$\ln(N_{air}) = 6.667 - 0.00133\,T - 1.687\,\ln(\varepsilon_a - 0.15), \quad (13b)$$

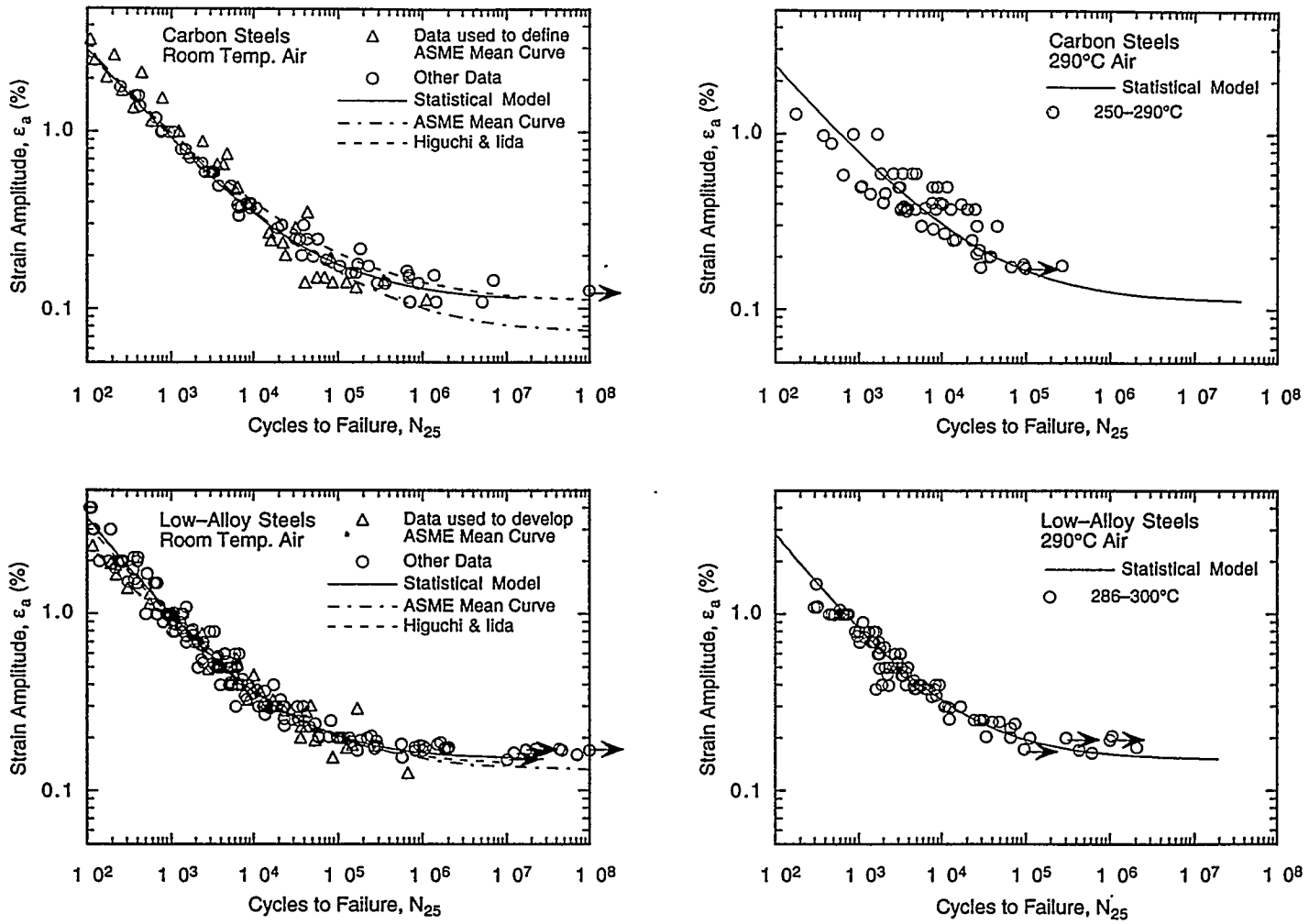

Figure 3. Fatigue S–N behavior for carbon and low–alloy steels in air at room temperature and 290°C

where ε_a is the strain amplitude (%) and T is the temperature (°C). The fatigue lives of CSs and LASs in air at room temperature and 288°C are compared with the values estimated from Eqs. 13a and 13b in Fig. 3. The results indicate significant heat–to–heat variation. At 288°C, fatigue life may vary by up to a factor of 5 above or below the mean value. The results also indicate that the ASME mean curve for CSs is not consistent with the experimental data; at strain amplitudes <0.2%, the mean curve predicts significantly lower fatigue lives than those observed experimentally. The estimated curve for LASs is comparable with the ASME mean curve. For both steels, Eq. 13 shows good agreement with the average curves of Higuchi and Iida [8], i.e., Eqs. 1a and 1b.

The fatigue data in LWR environments indicate a significant decrease in fatigue life of CSs and LASs when five conditions are satisfied simultaneously, i.e., when applied strain range, service temperature, DO in the water, and S content of the steel are above minimum threshold levels, and loading strain rate is below a threshold value. Although the microstructures and cyclic–hardening behavior of CSs and LASs are significantly different, environmental degradation of fatigue life of these steels is identical. For service conditions that satisfy all critical threshold values, the fatigue life of CSs is expressed as

$$\ln(N_{water}) = 6.186 - 1.871 \ln(\varepsilon_a - 0.11) + 0.554\ S^* T^* O^*\ \dot{\varepsilon}^* \qquad (14a)$$

and that of LASs as

$$\ln(N_{water}) = 5.901 - 1.687 \ln(\varepsilon_a - 0.15) + 0.554\ S^* T^* O^*\ \dot{\varepsilon}^*, \qquad (14b)$$

where S^*, T^*, O^*, and $\dot{\varepsilon}^*$ = transformed S content, temperature, DO, and strain rate, respectively, defined as follows:

$$\begin{aligned} S^* &= S && (0 < S \le 0.015 \text{ wt.\%} \\ S^* &= 0.015 && (S > 0.015 \text{ wt.\%}) \end{aligned} \qquad (15a)$$

$$\begin{aligned} T^* &= 0 && (T < 150°C) \\ T^* &= T - 150 && (T = 150–350°C) \end{aligned} \qquad (15b)$$

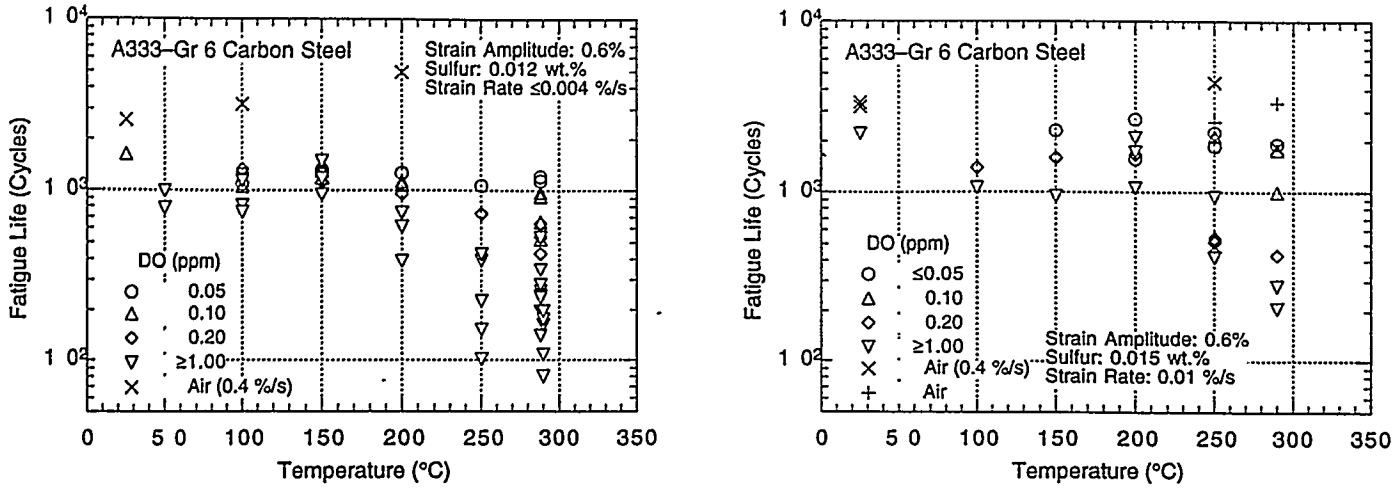

Figure 4. Change in fatigue life of A333–Gr 6 carbon steel with temperature and DO

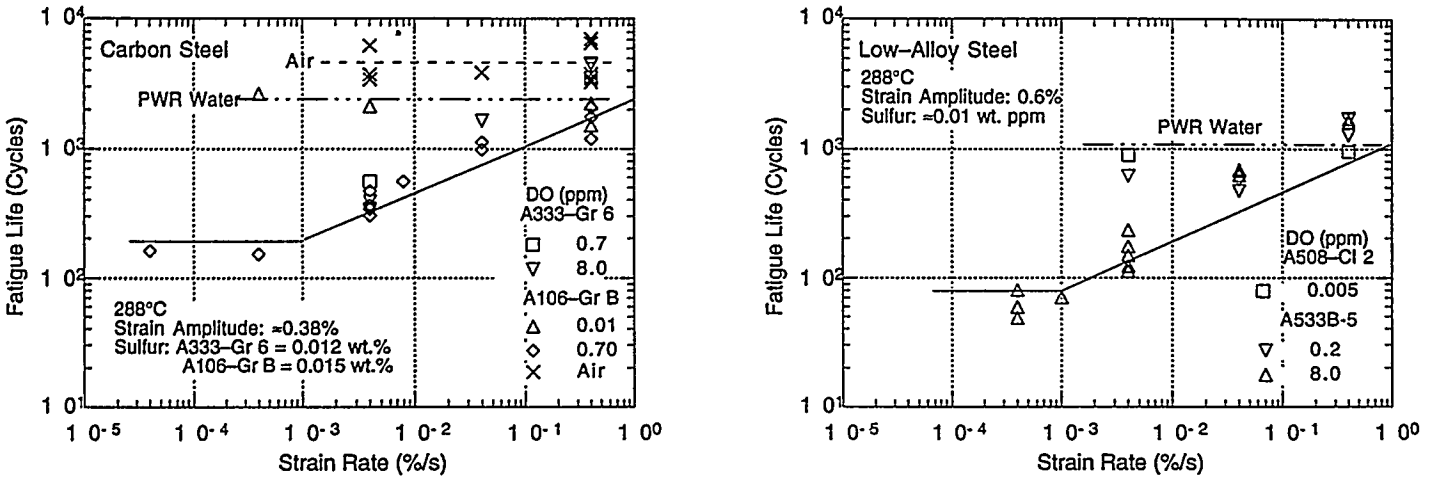

Figure 5. Dependence of fatigue life of several heats of carbon and low–alloy steels on strain rate at several DO levels

$O^* = 0$ (DO <0.05 ppm)
$O^* = DO$ (0.05 ppm ≤DO ≤0.5 ppm)
$O^* = 0.5$ (DO >0.5 ppm) (15c)

$\dot{\varepsilon}^* = 0$ ($\dot{\varepsilon}$ >1 %/s)
$\dot{\varepsilon}^* = \ln(\dot{\varepsilon})$ (0.001 ≤$\dot{\varepsilon}$ ≤1 %/s)
$\dot{\varepsilon}^* = \ln(0.001)$ ($\dot{\varepsilon}$ <0.001 %/s). (15d)

The functional forms for S^*, T^*, O^*, and $\dot{\varepsilon}^*$ were defined on the basis of the experimental data. The change in fatigue life of A333–Gr 6 CS with test temperature at different levels of DO [8–11] is shown in Fig. 4. Other parameters, e.g., strain amplitude, strain rate, and S content in steel, were kept constant; the applied strain amplitude and S content were above and strain rate was below the critical threshold values. The results indicate a threshold temperature of 150°C, above which environment decreases fatigue life if DO in water is also above the critical threshold level. In the temperature range of 150–320°C, fatigue life decreases linearly with temperature; the decrease s greater at high temperatures and DO levels.

The S–N data indicate that strain rates above 1%/s have little or no effect on fatigue life of CSs and LASs in LWR environments. For strain rates <1%/s, fatigue life decreases rapidly with decreasing strain rate. The fatigue lives of several heats of CSs and LASs [1–4,8–10] are plotted as a function of strain rate in Fig. 5. As noted before, the strain rate during tensile loading cycle is considered to be important for environmental effects on fatigue life. The results indicate that when all of the threshold conditions are satisfied, fatigue life decreases with decreasing strain rate and increasing levels of DO in water and S content in the steel. For both CSs and LASs, fatigue life appears to saturate at a strain rate of ≈0.001%/s.

The dependence of fatigue life of CSs on DO content in water [9–11] is shown in Fig. 6. The test temperature, applied strain amplitude, and S content in steel were above, and strain rate was below, the critical threshold values. The results indicate that for DO above 0.05 ppm, fatigue life of the steel decreases and that fatigue life saturates at 0.5 ppm, i.e., increases in DO levels above 0.5 ppm do not cause further decreases in fatigue life. In Fig. 6, for DO levels

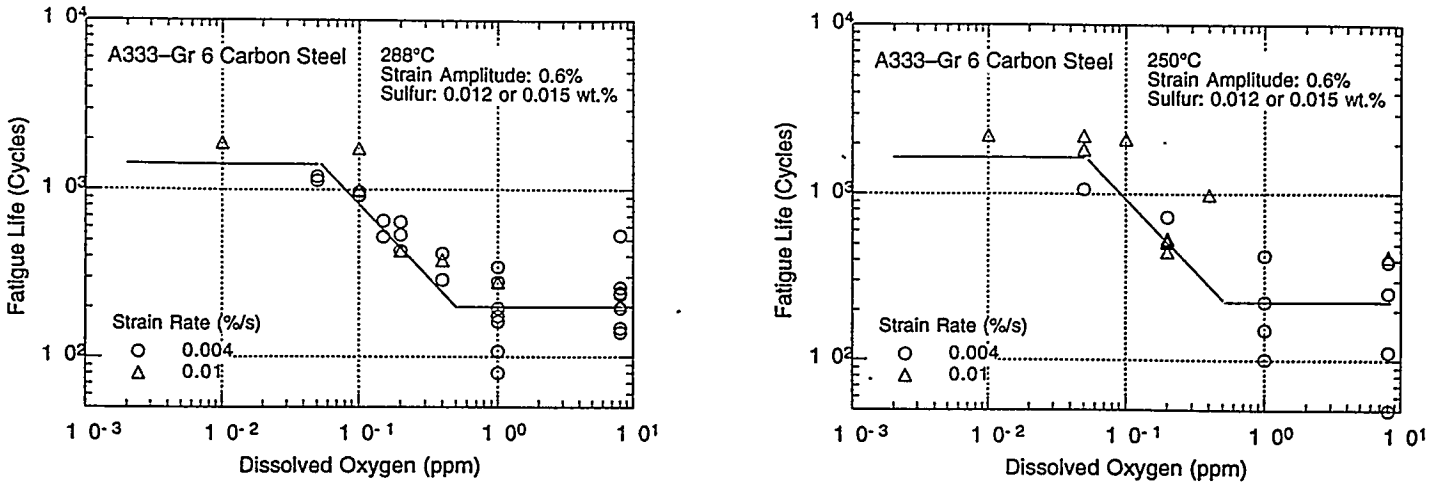

Figure 6. Dependence on DO of fatigue life of carbon steel

between 0.05 and 0.5 ppm, fatigue life decreases logarithmically with DO. However, because of the large scatter in the data, it is difficult to define the functional form for the dependence of life on DO content. A linear dependence of life on DO content was used in the model. The available data are inadequate to establish either the dependence of fatigue life on S content or the upper limit for S content above which the effect of S on fatigue life saturates. A linear dependence of life on S content was used in the model; the effect of S was assumed to saturate at 0.015 wt.%.

Experimental fatigue lives of CSs and LASs in water and those estimated from Eqs. 14a and 14b are plotted in Fig. 7. For both steels, environmental effects on fatigue life are minimal when the last term in Eqs. 14a and 14b is zero, e.g., in low–DO PWR environments. The predicted fatigue lives show good agreement with the experimental results.

The statistical model can be used to obtain a correction factor F_{en} to incorporate the effect of LWR coolant environment on fatigue life of carbon and low–alloy steels. The expression for fatigue life correction factor (Eq. 2) can be written in the form

$$\ln(F_{en}) = \ln(N_{air}) - \ln(N_{water}). \tag{16}$$

The correction factor is obtained by subtracting Eqs. 14a and 14b from Eqs. 13a and 13b, respectively. Thus, for CSs

$$F_{en} = \exp\left(0.384 - 0.00133T - 0.554S^*T^*O^*\dot{\varepsilon}^*\right) \tag{17a}$$

and for LASs

$$F_{en} = \exp\left(0.766 - 0.00133T - 0.554S^*T^*O^*\dot{\varepsilon}^*\right). \tag{17b}$$

An environmental fatigue correction factor F_{en} based on Eqs. 17a and 17b has been proposed by the Electric Power Research Institute (EPRI) for ASME Code Section III, NB–3600– and NB–

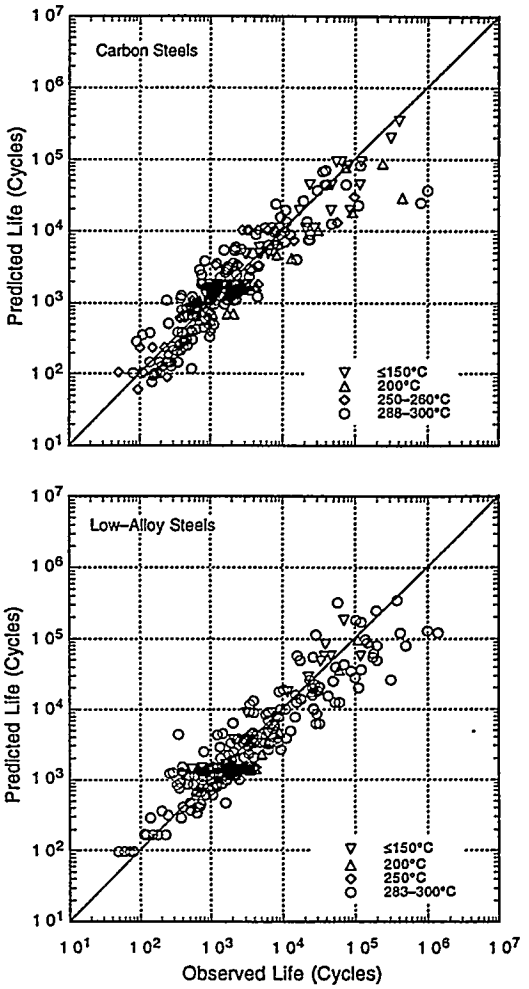

Figure 7. Fatigue lives of carbon and low–alloy steels estimated from the statistical model and determined experimentally in water

3200–type fatigue analysis [12]. The critical threshold conditions have also been defined to eliminate load–state pairs for which environmental correction is not necessary. Only those load–state pairs that satisfy all of the threshold conditions were used in evaluating an environmental correction factor. An environmental correction factor is necessary if all of the following threshold conditions are satisfied: strain amplitude >0.1%, strain rate <0.1%/s, DO level >0.1 ppm, temperature >150°C, S content in steel ≥0.003 wt.%, and fluid velocity ≤3 m/s. The proposed approach was applied to several examples, including BWR feedwater piping, recirculating piping, and a feedwater nozzle safe end.

CRACK PROPAGATION MODEL

The fatigue S–N curves specify, for a given strain or stress amplitude, the number of cycles needed to form an "engineering" crack (e.g., a 3–mm–deep crack). The allowable number of cycles can be divided into two stages: cycles for formation of microcracks on the surface (Stage I cracks), and cycles for propagation of the shallow surface cracks to an engineering size (Stage II cracks). At low strain ranges (i.e., high–cycle fatigue), life is dominated by the nucleation of surface microcracks, whereas at high strain ranges (i.e., low–cycle fatigue), the crack propagation phase dominates. Crack nucleation life is controlled by the strength of the material and is assumed to depend primarily on the applied stress range (or elastic strain range). Crack propagation life is controlled by ductility of the material and depends primarily on applied plastic strain range. The effect of LWR coolant environment on the formation of surface cracks is expected to differ from that for crack propagation. The fatigue crack growth behavior of ferritic steels in high–temperature oxygenated water and the effects of S content and loading rate are well known [13–15]. Dissolution of MnS inclusions changes the water chemistry near the crack tip, making it more aggressive. This results in enhanced crack growth rates (CGRs). Limited data indicate that environment appears to have little or no effect on crack nucleation [1–3]. Although all of the specimens tested in water show surface micropitting, there is no indication that these micropits facilitate the formation of surface cracks. Irrespective of environment, cracks in carbon and low–alloy steels form either along slip bands, carbide particles, or at the ferrite/pearlite phase boundaries.

A fracture mechanics approach for elastic–plastic materials has been used to incorporate environmental effects into the fatigue S–N curves with enhanced CGR (da/dN) data [16,17]. By characterizing the growth behavior of short cracks in terms of ΔJ, fracture mechanics analysis can be used to derive low–cycle fatigue relationships [18,19]. In this approach, the basic assumptions are that fatigue life can be represented by the number of cycles required for a crack to grow from an initial microscopic size to the final engineering size, and the CGR is controlled by ΔJ imposed during opening of the crack surface. This implies that the J–integral defines the nonlinear stress and strain fields near the crack tip during the loading half of the cycle despite intermittent unloading. The value of ΔJ for elastic–plastic conditions is given by

$$\Delta J = \Delta J_e + \Delta J_p. \tag{18}$$

The elastic–plastic J value for a short crack is expressed as

$$J = \frac{K}{E_l} + h(n,g)\sigma_l \varepsilon_p a, \tag{19}$$

where K is stress intensity parameter, $E_l = E$ for plane stress and $E_l = E/(1-\upsilon^2)$ for plane strain, E is the elastic modulus, υ is Poisson's ratio, σ_l is the nominal stress in a section away from the crack, ε_p is nominal plastic strain, a is crack length, and h(n,g) is a function of the strain hardening coefficient n in Eq. 20, and geometry g. The cyclic stress–strain curve is defined as

$$\varepsilon = \frac{\sigma}{E} + \left(\frac{\sigma}{A}\right)^n, \tag{20}$$

where ε and σ are cyclic strain and stress amplitudes, respectively, n is the strain hardening coefficient, and A is a constant. Three–dimensional finite–element models have been used to evaluate the stress intensities associated with cracks in smooth cylindrical fatigue specimens [20], but a simple estimate of J for a small half–circular surface crack [18] is given by

$$J = 3.2\left(\frac{\sigma^2}{2E}\right)a + 5.0\left(\frac{\sigma\varepsilon_p}{1+n}\right)a. \tag{21}$$

This estimate of J is based on the assumption that the smooth cylindrical fatigue specimen can be represented as a semi–infinite space containing an edge crack and that the strain is considered to be in the fully plastic regime and uniformly applied remote from the crack. The estimates are good as long as the crack size is small compared to the specimen diameter. For conventional fatigue tests, i.e., fatigue life defined as the number of cycles for the tensile stress to drop 25% from its peak value, the crack depth–to–specimen diameter ratio can be as high as 0.4. More rigorous finite–element models can be used to modify the stress intensities associated with conventional fatigue test specimens.

Section XI of the ASME Boiler and Pressure Vessel Code provides CGR curves for carbon and low–alloy steels. The growth rate da/dN (in micro–inches/cycle) in air is given by

$$\frac{da}{dN} = 1.99\times10^{-10}(\Delta K)^{3.07} \tag{22a}$$

where the stress intensity factor range $\Delta K = K_{max} - K_{min}$ (ksi$\sqrt{}$in.). In reactor water environments, the growth rates at low ΔKs are given by

$$\frac{da}{dN} = 1.02\times10^{-12}(\Delta K)^{5.95} \tag{22b}$$

and at high ΔKs by

$$\frac{da}{dN} = 1.01\times10^{-7}(\Delta K)^{1.95}. \tag{22c}$$

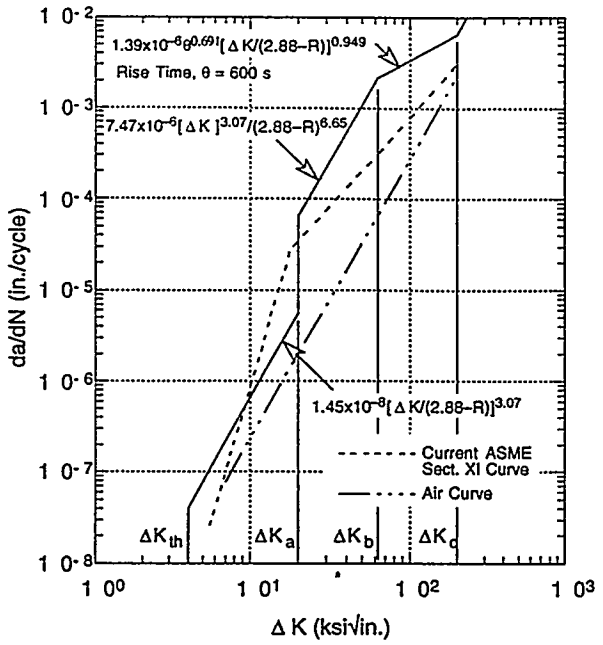

Figure 8. Proposed reference fatigue crack growth rate curves for carbon and low–alloy steels in water environments for a rise time of 600 s and R = –1

The current ASME Section XI reference curves for CGRs are based on fatigue data obtained prior to 1980; all fatigue tests were conducted at a rate of 1 cycle/min. Recent experimental results have shown the importance of key variables of material, environment, and loading rate on CGRs in LWR environments. Fatigue CGR correlations, shown in Fig. 8, have been developed that explicitly consider the effects of rise time, R–ratio, ΔK, and S content in the steel [21,22]. The new CGR correlations can be divided into two categories. For low–S behavior, CGRs are faster by a factor of ≈2 in reactor water than the corresponding rates in air. For high–S behavior or when environmentally assisted cracking (EAC) occurs, CGRs are defined as a function of rise time θ, R–ratio, and stress intensity range ΔK. The threshold value of ΔK below which CGRs are negligible is given by

$$\begin{aligned} \Delta K_{th} &= 4.0\,(1-R) && 0 \le R \le 0.75 \\ &= 1.0 && 0.75 < R < 1. \end{aligned} \quad (23a)$$

The threshold value for EAC ΔK_a above which the CGR is enhanced by the environment, is given by

$$\begin{aligned} \Delta K_a &= 0.376\,\theta^{0.125}\,(2.88-R)^{2.99} && 0 \le R \le 0.9 \\ &= 2.900\,\theta^{0.125}\,\exp[(0.9-R)/(1.0-R)] && 0.9 < R < 1, \end{aligned} \quad (23b)$$

where θ is the rise time in sec. The values of ΔK_b and ΔK_c that delineate regions of enhanced CGR are given by

$$\begin{aligned} \Delta K_b &= 0.453\,\theta^{0.326}\,(2.88-R)^{2.69} \\ \Delta K_c &= 8.570\,\theta^{0.326}\,(2.88-R). \end{aligned} \quad (23c)$$

For K_{min} <0. e.g., fully reversed cyclic loading, R is set equal to zero. The correlations of Fig. 8 and Eqs. 21 and 23 have been used to derive the S–N curves of carbon and low–alloy steels under different loading conditions, including the effect of mean stress [17]. The correlations have also been used to account for the effect of the environment and strain rate on the fatigue life of small specimens [5]. The results of the analysis show that there exists a saturation strain rate below which fatigue life does not decrease with decreasing strain rate; indeed, it is possible that there is recovery or an increase in life at strain rates below the critical value.

SLIP DISSOLUTION MODEL

A model based on oxide film rupture and anodic dissolution has also been proposed to incorporate environmental effects on the fatigue life of carbon and low–alloy steels [23]. The requirements for this approach are that a protective oxide film is thermodynamically stable to ensure that a crack will propagate with a high aspect ratio without degrading into a blunt pit, and that a strain increment occurs to rupture that film, thereby exposing the underlying matrix to the environment. The environmentally assisted growth rate V is related to the crack tip strain rate $\dot{\varepsilon}_{ct}$ by the relationship

$$V = A(\dot{\varepsilon}_{ct})^n, \quad (24a)$$

where V is in cm s^{-1}, $\dot{\varepsilon}_{ct}$ is in s^{-1}, and the constants A and n depend on the material and environmental conditions at the crack tip. There is a lower limit of crack propagation rate associated either with blunting when the crack tip cannot keep up with general corrosion rate of the crack sides, or with the fact that a high dissolved S activity cannot be maintained at the crack tip. The critical crack propagation rate at which this transition occurs will depend on DO level, flow rate, etc. Based on these factors, the maximum and minimum environmentally controlled crack propagation rates have been defined [23]. For crack–tip S concentrations >2 ppm,

$$V = 2.25\times10^{-4}\,\dot{\varepsilon}_{ct}^{\,0.35} \quad (24b)$$

and for crack–tip S concentrations <0.02 ppm by

$$V = 10^{-2}\,\dot{\varepsilon}_{ct}^{\,1.0}. \quad (24c)$$

The model assumes that there is no environmental enhancement of crack propagation during the compressive load cycle, because during that period the water does not have access to the crack tip. The total crack advance per cycle Δa_{total} is given by the summation of crack advance in air Δa_{air} due to mechanical factors, and crack advance from a slip–dissolution mechanism Δa_r, once the tensile strain increment exceeds the fracture strain of the oxide ε_f. If the fatigue life is considered to represent the number of cycles required to form a 3–mm–deep crack, the crack advance per loading cycle in air is given by $0.3/N_{air}$. The fatigue life in air can be expressed by Eqs. 1, 6, or 13. Thus, assuming that environmental conditions are such as to maintain >2 ppm S at the crack tip (Eq. 24a) and that the crack–tip strain rate $\dot{\varepsilon}_{ct}$ is the same as the applied strain rate $\dot{\varepsilon}_{app}$, the environmental increment in crack growth is given by integrating Eq. 24a

$$\Delta a_r = \int_0^{a_r} da = \int_{\varepsilon_f/\dot{\varepsilon}}^{t_r} 2.25\text{x}10^{-4}\left(\dot{\varepsilon}_{app}\right)^{0.35} dt \qquad (25a)$$

or

$$\Delta a_r = 2.25\text{x}10^{-4}\left(\dot{\varepsilon}_{app}\right)^{0.35}\left(\frac{\Delta\varepsilon}{\dot{\varepsilon}_{app}} - \frac{\varepsilon_f}{\dot{\varepsilon}_{app}}\right), \qquad (25b)$$

where the relevant time for integration is the rise time t_r minus the time taken for the strain increment to exceed the fracture strain of the oxide $\left(\varepsilon_f/\dot{\varepsilon}_{app}\right)$. Thus, the total crack advance per cycle is given by

$$\Delta a_{total} = \Delta a_{air} + \Delta a_r = \frac{0.3}{N_{air}} + 2.25\text{x}10^{-4}\left(\Delta\varepsilon - \varepsilon_f\right)\left(\dot{\varepsilon}_{app}\right)^{-0.65}, \qquad (26)$$

where crack advance is in cm and strain rate $\dot{\varepsilon}_{app}$ is in s^{-1}. The fatigue life in water N_{water} is given by the initiation crack depth (3 mm) divided by the total crack advance per cycle Δa_{total}

$$N_{water} = 0.3\Big/\left[\frac{0.3}{N_{air}} + 2.25\text{x}10^{-4}\left(\Delta\varepsilon - \varepsilon_f\right)\left(\dot{\varepsilon}_{app}\right)^{-0.65}\right]^{-1}. \qquad (27)$$

The fatigue lives estimated from Eqs. 27 and 14, and those observed experimentally for A333–Gr 6 steel in 8 ppm DO water at 250°C and various strain rates, are shown in Fig. 9. These estimates are based on the assumption that a high–S concentration can be maintained at the crack tip, i.e., Eq. 24a is applicable. The estimated and observed change in relative fatigue life (i.e., N_{water}/N_{air}) with strain rate for A106–Gr B steel in 288°C water is shown in Fig. 10. The estimated curves for high– and low–S concentration are based on Eqs. 24a and 24b, respectively. In this case, the relative life decreases with decreasing strain rate up to a point where the crack propagation rate can not maintain a high dissolved S concentration at the crack tip. At strain rates below this point, the crack propagation rate is controlled by the low–S concentration relationship given by Eq. 24b. The predicted transition [23] for a corrosion potential of +200 mVshe (8 ppm DO) is shown in the figure. Although both crack propagation and slip–dissolution models predict recovery in life at very low strain rates, limited data suggest saturation at ≈0.001%/s strain rate rather than an increase in life at strain rates. below the critical value

FATIGUE DESIGN CURVES

The current ASME Section III Code design fatigue curves were based on a best–fit curve to the experimental data expressed in terms of stress amplitude S_a and fatigue cycles N. The RT value of 206.8 GPa (30,000 ksi) for the elastic modulus was used to convert the experimental strain–vs.–life data to stress–vs.–life curves. The best–fit curves were adjusted for the effect of mean stress by using the modified Goodman relation

$$S_a' = S_a\left(\frac{\sigma_u - \sigma_y}{\sigma_u - S_a}\right) \qquad \text{for } S_a < \sigma_y, \qquad (28a)$$

and

$$S_a' = S_a \qquad \text{for } S_a > \sigma_y, \qquad (28b)$$

where S_a' is the adjusted value of stress amplitude, and σ_y and σ_u are the yield and ultimate strengths of the material, respectively. The design fatigue curves were then obtained by lowering the adjusted best–fit curve by a factor of 2 on stress or 20 on cycles, whichever was more conservative, at each point on the curve. The factor of 20 on cycles was intended to account for the uncertainties in fatigue life associated with material and loading conditions, and the factor of 2 on strain was intended to account for uncertainties in threshold strain caused by material variability. The interim design curves [5] were also developed by the same procedure. However, instead of a single curve, a family of best–fit experimental curves that vary with specific loading and environmental conditions was used.

In the present study, the best–fit or mean curve to the experimental data given by the statistical models has been used to develop fatigue design curves for components. First, the mean curve is

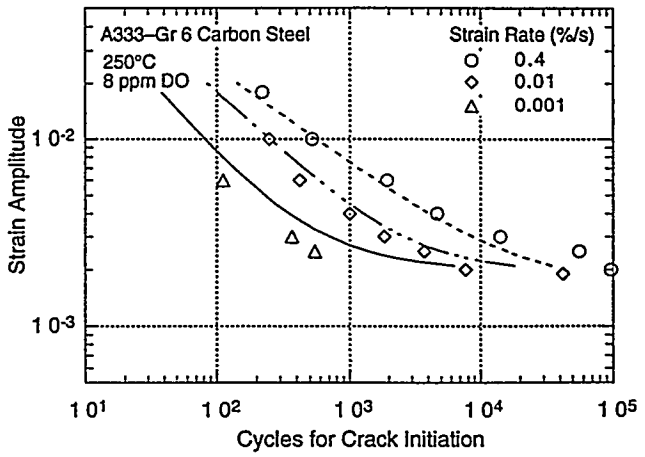

Figure 9. Fatigue S–N behavior for A333–Gr 6 carbon steel estimated from the slip–dissolution model and determined experimentally in 250°C water

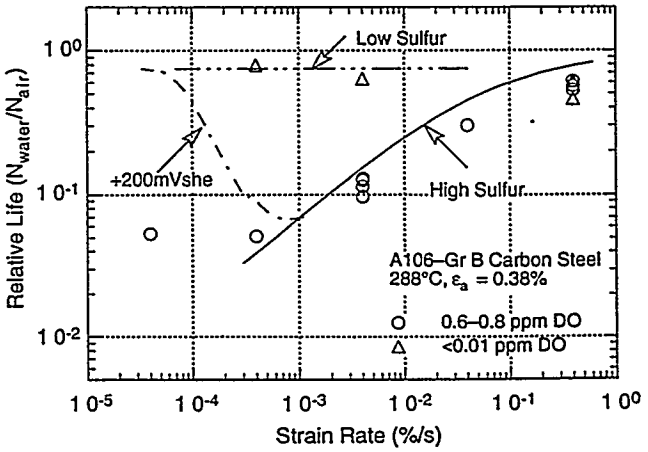

Figure 10. Comparison between observed and predicted N_{water}/N_{air} vs. strain rate relationship for A106–Gr B steel in water

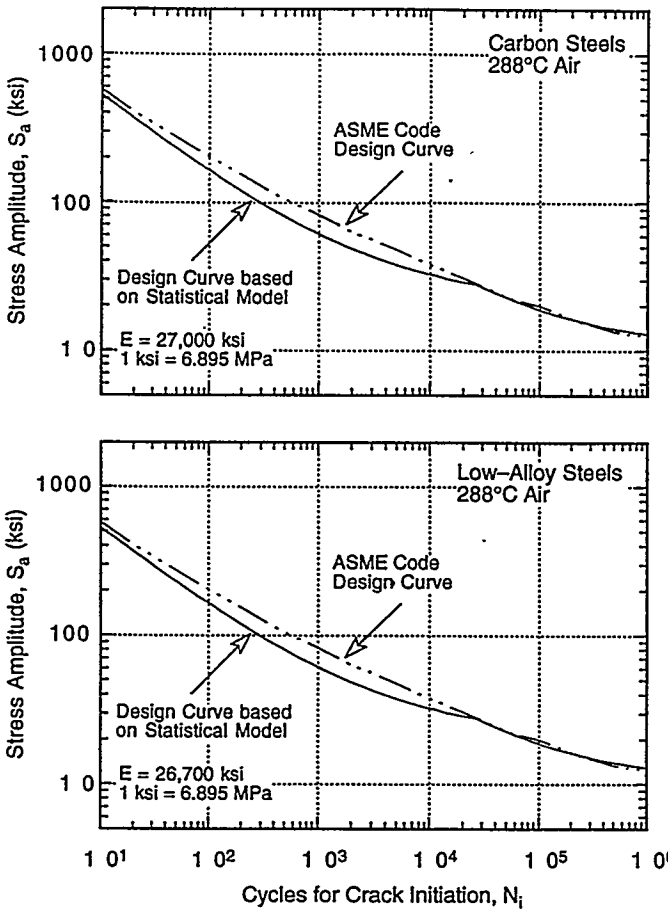

Figure 11. Fatigue design curves developed from tstatistical model for carbon and low–alloy steels in 288°C air

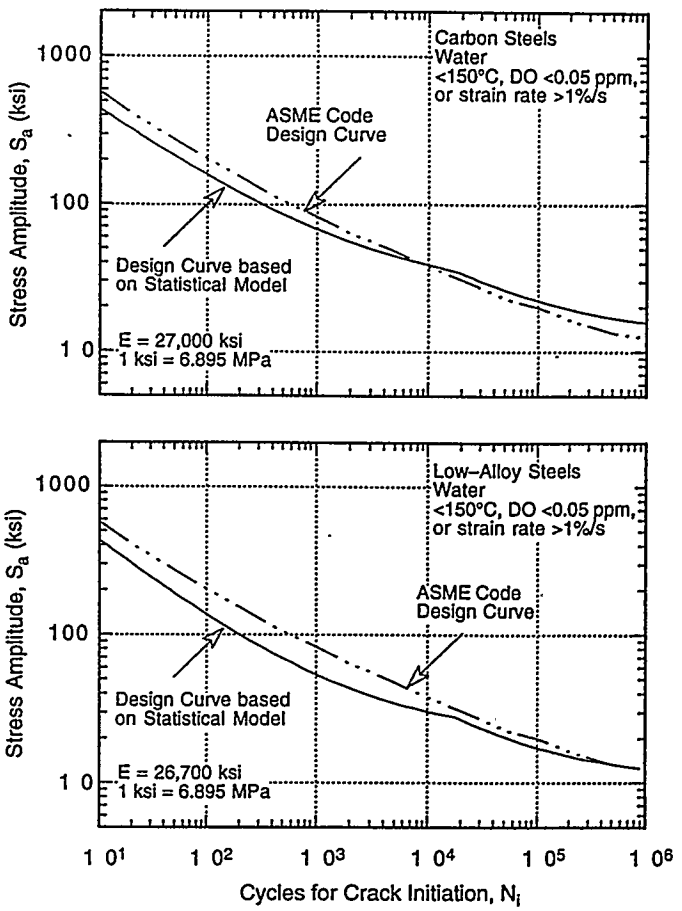

Figure 12. Fatigue design curves developed from tstatistical model for carbon and low–alloy steels under service conditions where one or more critical threshold values are not satisfied

adjusted for the effect of mean stress by using the Goodman relation of Eq. 28. Note that the Goodman relation assumes the maximum possible mean stress and typically gives a conservative adjustment for mean stress, at least when environmental effects are not significant. For CSs and LASs, the values of elastic modulus and tensile properties were the same as those used in adjusting the ASME Code design curve, e.g., the cyclic yield and ultimate strengths at room temperature, respectively, were 276 and 552 MPa (40 and 80 ksi) for CS and 483 and 689 MPa (70 and 100 ksi) for LAS. The mean–stress–adjusted fatigue life in air of CSs is expressed as

$$\ln(N_{air}) = 6.582 - 0.00133\,T - 2.032\,\ln(\varepsilon_a - 0.094) \qquad (29a)$$

and that of LASs as

$$\ln(N_{air}) = 6.857 - 0.00133\,T - 1.813\,\ln(\varepsilon_a - 0.080). \qquad (29b)$$

The mean–stress–adjusted fatigue life in water of CSs is expressed as

$$\ln(N_{water}) = 6.198 - 2.032\,\ln(\varepsilon_a - 0.094) + 0.554\,S^*T^*O^*\,\dot{\varepsilon}^* \qquad (30a)$$

and that of LASs as

$$\ln(N_{water}) = 6.091 - 1.813\,\ln(\varepsilon_a - 0.080) + 0.554\,S^*T^*O^*\,\dot{\varepsilon}^*. \qquad (30b)$$

The fatigue design curves for carbon and low–alloy steels in 288°C air and for service conditions where one or more critical threshold conditions is not satisfied are shown in Figs. 11 and 12, respectively. In air environment, the design curves developed from the statistical model are somewhat different than the ASME Code curve because of temperature effects. The statistical model curves are for 288°C air and are based on the elastic modulus at temperature, whereas the Code curve is for room temperature. Figure 12 shows that environmental effects are negligible when any one of the threshold conditions is not satisfied, e.g., at temperatures below 150°C or in a low–DO PWR environment.

The fatigue design curves adjusted for environmental effects in water at 200, 250, and 288°C are shown in Fig. 13. The design curve corresponding to the saturation strain rate of 0.001%/s is shown in the figure; similar curves can be obtained for other strain rates. A high–S content is assumed in the steels, e.g., 0.015 wt.% or higher. Because

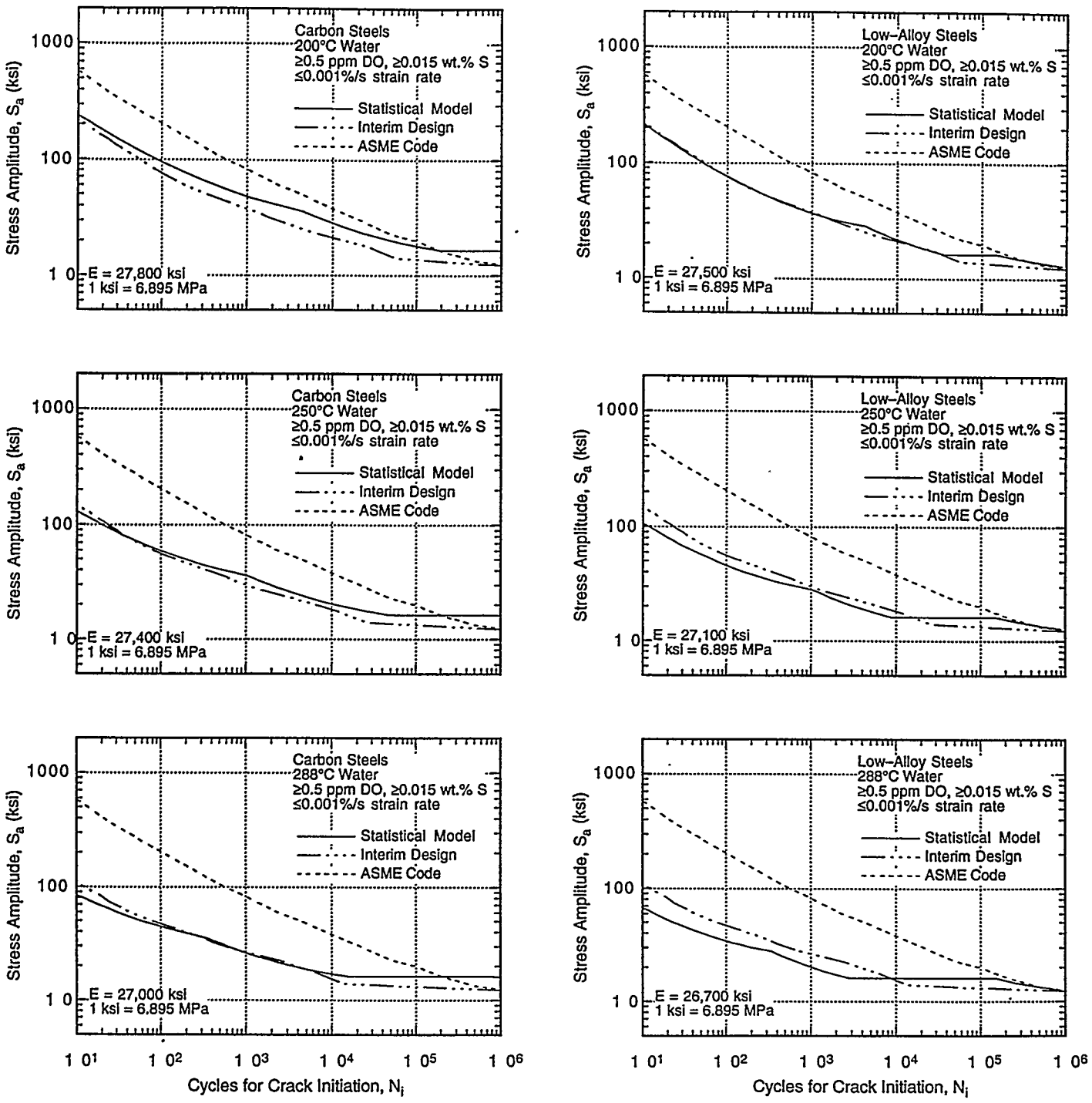

Figure 13. Fatigue design curves developed from statistical model for carbon and low-alloy steels under service conditions where all critical threshold values are satisfied

the functional form for dependence of fatigue life on DO content is not well established, a DO level of 0.5 ppm was used in these calculations. This is expected to be a conservative estimate of environmental effects with respect to the nominal DO level of 0.2 ppm for BWRs operating with normal water chemistry. Additional data are needed before a better estimate can be made. Also, a threshold strain amplitude for environmental effects is estimated to be 0.06%. Limited data indicate that the threshold strain is ≈20% higher than the fatigue endurance limit of the steel; a threshold strain amplitude of 0.18% was observed for two heats of CSs and LASs [1,3]. A threshold value of 0.06% is obtained

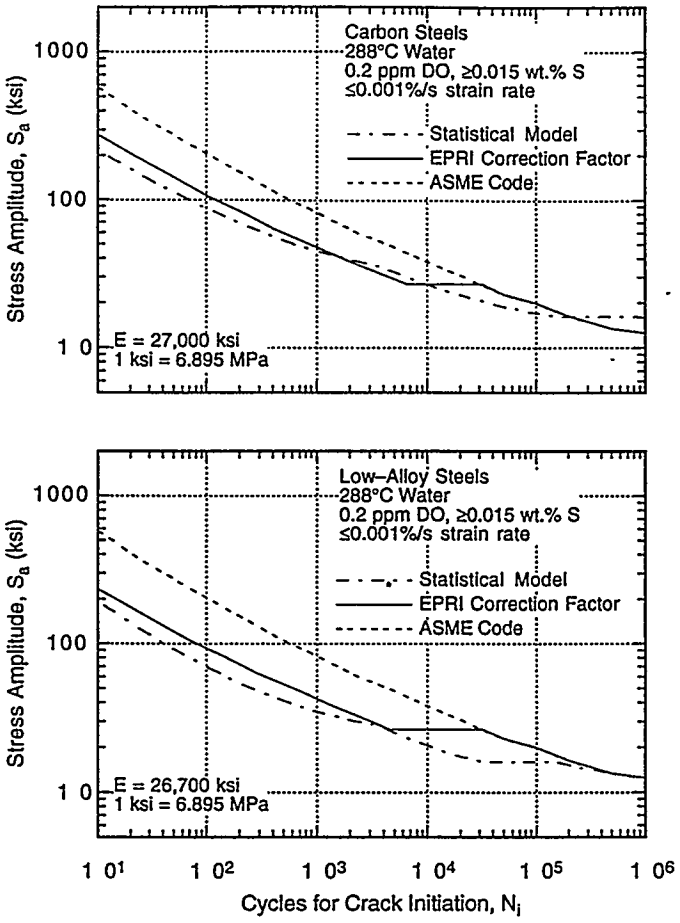

Figure 14. Fatigue design curves based on fatigue life correction factor proposed by EPRI for carbon and low–alloy steels in 288°C water

after adjusting for the effects of mean stress and material variability. Statistical analysis of the existing fatigue S–N data indicate that a factor of 1.7 on strain provides a 95% confidence for the variations in life associated with material variability [6]. For both steels, the design curves of Fig. 12 are used at strain amplitudes below the threshold value of 0.06%.

Figure 14 shows the fatigue design curves for CSs and LASs determined by applying a environmental correction factor proposed by EPRI to the ASME Code curve and those obtained from the statistical model. The curves correspond to an S content of ≥0.015 wt.%, saturation strain rate of 0.001%/s, and nominal DO level of 0.2 ppm for BWRs. These service conditions yield a correction factor F_{en} of 4.88 and 7.15 (from Eq. 17) for CSs and LASs, respectively. The main difference between the EPRI approach and the design curves determined from the statistical model is the value of threshold strain amplitude for environmental effects. The EPRI approach uses a mean value of 0.1% for the threshold strain, which has not been adjusted for the effects of mean stress or material variability.

FATIGUE EVALUATION

The various fatigue S–N correlations and models show good agreement with data obtained under loading histories with constant strain rate, temperature, and strain amplitude. Actual loading histories are far more complex. Exploratory fatigue tests have been conducted with waveforms where the strain rate or temperature was varied during the loading cycle. The results of such tests provide guidance for developing procedures and rules for fatigue evaluation of components under complex loading histories.

For loading cycles in which strain rate and temperature also vary with strain, the results show two different trends. The data for A106–Gr B steel at 0.75% strain range suggest that environmental effects on fatigue life occur only when the threshold conditions are satisfied [3,4]. A typical hysteresis loop for the tests is shown in Fig. 15. A slow strain rate is effective in decreasing fatigue life only when it occurs at strains greater than the threshold strain ε_{th}, i.e., during portion BA of the tensile loading cycle. The data also suggest that the slow strain rates applied during any portion of the loading cycle above the minimum threshold strain are equally effective in decreasing life. This behavior is consistent with the slip–dissolution model [23], i.e., the applied strain must exceed a threshold value to rupture the passive surface film in order for environmental effects to occur. In contrast, the data for A333–Gr 6 steel at 1.2% strain range with waveforms where the strain rate or temperature was varied during the loading cycle, suggest that all portions of the tensile loading cycle are equally damaging, including the portion where the applied strain is below the threshold value, i.e., portion CB in Fig. 15 [9,11].

Fatigue lives for loading histories where strain rate, temperature, and strain amplitude are changing can be estimated from the statistical model (Eqs. 13 and 14). If the temperature dependence of fatigue life in air is ignored, Eqs. 13a and 14a can be written as

$$\varepsilon_a = 33.52(N)^{-1/1.871} + 0.11 \qquad (31a)$$

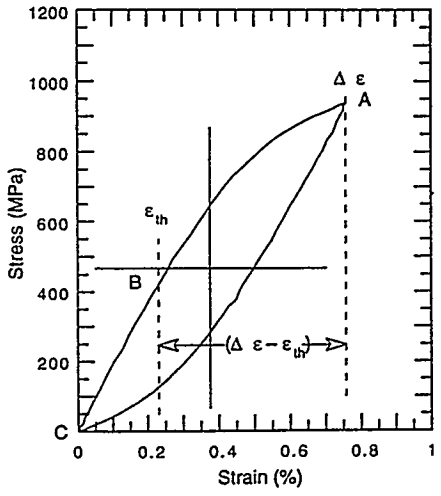

Figure 15. Typical hysteresis loop for fatigue test on A106–Gr B carbon steel in water at 288°C

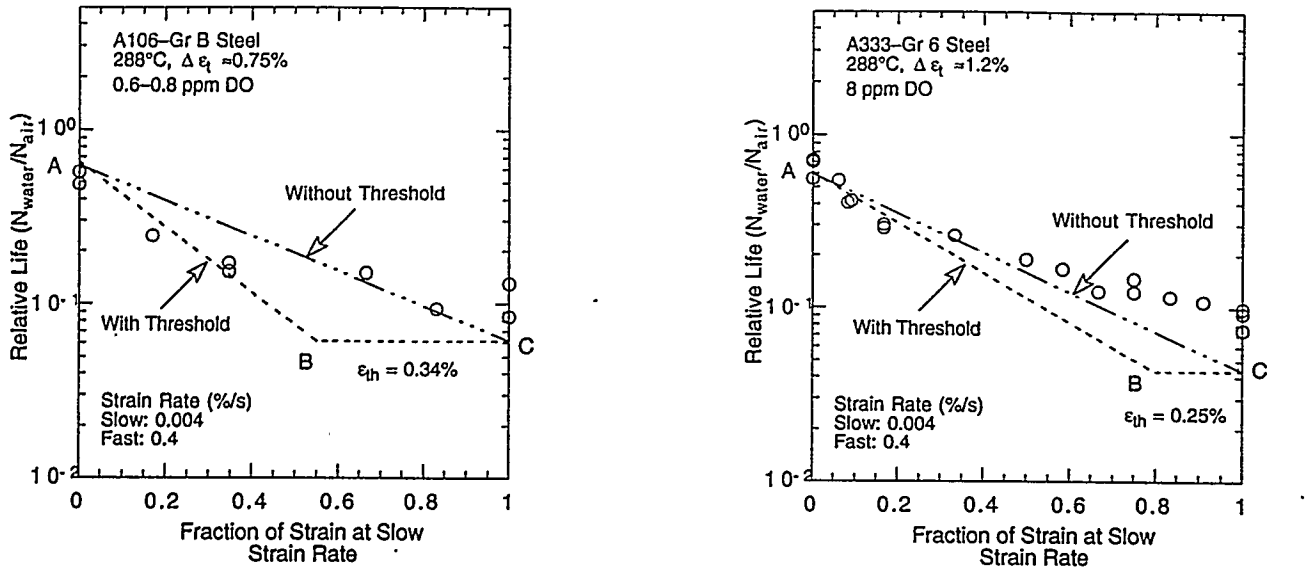

Figure 16. Experimental and estimated fatigue lives of A106–Gr B and A333–Gr 6 carbon steels at 288°C tested with waveforms where slow strain rate is applied during part of tensile loading cycle

and

$$\varepsilon_a = 27.28(N)^{-1/1.871}(\dot{\varepsilon})^{-0.554S^*T^*O^*/1.871} + 0.11, \quad (31b)$$

respectively. From the above equations, an equivalent strain amplitude in air that would yield the same life as in water can be defined as

$$\varepsilon_{aA} = (\varepsilon_{aW} - 0.11)(\dot{\varepsilon})^{-0.554S^*T^*O^*/1.871} + 0.11. \quad (32)$$

For loading histories with varying strain rate and temperature, Eq. 32 can be written as

$$\Delta\varepsilon_A = \sum_{\varepsilon_{th}}^{\Delta\varepsilon} \Delta\varepsilon_W(\dot{\varepsilon})^{-0.554S^*T^*O^*/1.871} + \varepsilon_{th} \quad (33a)$$

or

$$\Delta\varepsilon_A = \int_{\varepsilon_{th}}^{\Delta\varepsilon} (\dot{\varepsilon})^{1-(0.554S^*T^*O^*/1.871)}\, dt + \varepsilon_{th}, \quad (33b)$$

where ε_{th} is the threshold strain for environmental effects to occur.

Equation 33 can be used to estimate the fatigue life for tests conducted with waveforms where the tensile strain rate was varied during the loading cycle. The variation in fatigue life of carbon steels, estimated from Eq. 33, with and without a threshold strain, and that observed experimentally, is plotted as a function of the fraction of the loading strain at slow strain rate in Fig. 16 [1,3,9]. For both steels, the estimated values show good agreement with the experimental data. Equation 33 can also be used to estimate the fatigue life for loading histories with varying strain rate and temperature.

CONCLUSIONS

Several correlations and models have been presented for estimating the effects of LWR coolant environments on fatigue S–N curves for carbon and low–alloy steels, and the results are compared with experimental data. The statistical model provides a good basis for developing fatigue design curves and procedures that incorporate the effect of LWR coolant environments on the fatigue life of carbon and low–alloy steels. The best–fit or mean curve to the experimental data given by the statistical model has been used to develop fatigue design curves that take into account temperature, DO in water, S content in steel, and strain rate. Estimations of fatigue lives under complex loading histories are discussed. Fatigue lives for loading histories where strain rate, temperature, and strain amplitude are changing can be estimated from the statistical model.

ACKNOWLEDGMENTS

This work was supported by the Office of Nuclear Regulatory Research of the U.S. Nuclear Regulatory Commission, under FIN Number W6610; Program Manager: Dr. M. McNeil.

REFERENCES

1. Chopra, O. K., and Shack, W. J., "Effects of LWR Environments on Fatigue Life of Carbon and Low–Alloy Steels," in Fatigue and Crack Growth: Environmental Effects, Modeling Studies, and Design Considerations, PVP Vol. 306, S. Yukawa, ed., American Society of Mechanical Engineers, New York, pp. 95–109, 1995.

2. Chopra, O. K., and Shack, W. J., "Effects of Material and Loading Variables on Fatigue Life of Carbon and Low–Alloy Steels in LWR Environments," in Transactions of 13th Int. Conf. on Structural Mechanics in Reactor Technology (SMiRT 13),

Vol. II, M. M. Rocha and J. D. Riera, eds., Escola de Engenharia – Universidade Federal do Rio Grande do Sul, Porto Alegre, Brazil, pp. 551–562, 1995.

3. Chopra, O. K., and Shack, W. J., "Low–Cycle Fatigue of Piping and Pressure Vessel Steels in LWR Environments," to be published in Nucl. Eng. Des.

4. Chopra, O. K., and Shack, W. J., "Evaluation of Effects of LWR Coolant Environments on Fatigue Life of Carbon and Low–Alloy Steels," to be published in Proc. of Symposium on Effects of the Environment on the Initiation of Crack Growth, ASTM STP 1298, American Society for Testing and Materials, Philadelphia, 1997.

5. Majumdar, S., Chopra, O. K., and Shack, W. J., "Interim Fatigue Design Curves for Carbon, Low–Alloy, and Austenitic Stainless Steels in LWR Environments," NUREG/CR–5999, ANL–93/3, April 1993.

6. Keisler, J., Chopra, O. K., and Shack, W. J., "Fatigue Strain–Life Behavior of Carbon and Low–Alloy Steels, Austenitic Stainless Steels, and Alloy 600 in LWR Environments," NUREG/CR–6335, ANL–95/15, Aug. 1995.

7. Van Der Sluys, W. A., and Yukawa, S., "Status of PVRC Evaluation of LWR Coolant Environmental Effects on the S–N Fatigue Properties of Pressure Boundary Materials," in Fatigue and Crack Growth: Environmental Effects, Modeling Studies, and Design Considerations, S. Yukawa, ed., American Society of Mechanical Engineers, New York, pp. 47–58, 1995.

8. Higuchi, M., and Iida, K., "Fatigue Strength Correction Factors for Carbon and Low–Alloy Steels in Oxygen–Containing High–Temperature Water," *Nucl. Eng. Des.* **129**, pp. 293–306, 1991.

9. Higuchi, M., Iida, K., and Asada, Y., "Effects of Strain Rate Change on Fatigue Life of Carbon Steel in High–Temperature Water," in Fatigue and Crack Growth: Environmental Effects, Modeling Studies, and Design Considerations, PVP Vol. 306, S. Yukawa, ed., American Society of Mechanical Engineers, New York, pp. 111–116,1995.

10. Nagata, N., Sato, S., and Katada, Y., "Low–Cycle Fatigue Behavior of Low–Alloy Steels in High–Temperature Pressurized Water," in Transactions of 10th Int. Conf. on Structural Mechanics in Reactor Technology, F, A. H. Hadjian, ed., American Association for Structural Mechanics in Reactor Technology, Anaheim, CA, 1989.

11. Nakao, G., Kanasaki, H., Higuchi, M., Iida, K., and Asada, Y., "Effects of Temperature and Dissolved Oxygen Content on Fatigue Life of Carbon and Low–Alloy Steels in LWR Water Environment," in Fatigue and Crack Growth: Environmental Effects, Modeling Studies, and Design Considerations, PVP Vol. 306, S. Yukawa, ed., American Society of Mechanical Engineers, New York, pp. 123–128, 1995.

12. Mehta, H. S., and Gosselin, S. R., "An Environmental Factor Approach to Account for Reactor Water Effects in Light Water Reactor Pressure Vessel and Piping Fatigue Evaluations," EPRI Report TR–105759, Dec. 1995.

13. Ford, F. P., and Andresen, P. L., "Stress Corrosion Cracking of Low–Alloy Pressure Vessel Steel in 288°C Water," in Proc. 3rd Int. Atomic Energy Agency Specialists' Meeting on Subcritical Crack Growth, NUREG/CP–0112, Vol. 1, pp. 37–56, Aug. 1990.

14. Scott, P. M., and Tice, D. R., "Stress Corrosion in Low–Alloy Steels," *Nucl. Eng. Des.* **119**, pp. 399–413, 1990.

15. Kassner, T. F., Shack, W. J., Ruther, W. E., and Park, J. H., "Environmentally Assisted Cracking of Ferritic Steels," in Environmentally Assisted Cracking in Light Water Reactors: Semiannual Report, April–September 1990, NUREG/CR–4667, Vol. 11, ANL–91/9, pp. 2–9, May 1991.

16. O'Donnell, W. J., "Synthesis of S–N and da/dN Life Evaluation Technologies," in Proc. ASME Pressure Vessel and Piping Conf., 88–PVP–10, June 19–23, 1988.

17. O'Donnell, T. P., and O'Donnell, W. J., "Cyclic Rate–Dependent Fatigue Life in Reactor Water," in Fatigue and Crack Growth: Environmental Effects, Modeling Studies, and Design Considerations, PVP Vol. 306, S. Yukawa, ed., American Society of Mechanical Engineers, New York, pp. 59–69, 1995.

18. Dowling, N. E., "Crack Growth During Low–Cycle Fatigue of Smooth Axial Specimens," in Cyclic Stress–Strain and Plastic Deformation Aspects of Fatigue Crack Growth, ASTM STP 637, American Society for Testing and Materials, Philadelphia, pp. 97–121, 1977.

19. Mowbray, D. F., "Derivation of a Low–Cycle Fatigue Relationship Employing the J–Integral Approach to Crack Growth," in Cracks and Fracture, ASTM STP 601, American Society for Testing and Materials, Philadelphia, pp. 33–46, 1976.

20. O'Donnell, T. P., and O'Donnell, W. J., "Stress Intensity Values in Conventional S–N Fatigue Specimens," in Fatigue and Crack Growth: International Pressure Vessels and Piping Codes and Standards: Volume 1 – Current Applications, PVP Vol. 313–1, K. R. Rao and Y. Asada, eds., American Society of Mechanical Engineers, New York, pp. 195–197, 1995.

21. Eason, E. D., and Nelson, E. E., "Analysis of Fatigue Tests Propagation Data, A508 Class 2 and A533–B Steels in Light Water Reactor Environments," Draft Final Report on EPRI Project RP2006–20, MCS Report 891201, Dec. 1989.

22. Eason, E. D., Nelson, E. E., and Gilman, J. D., "Modeling of Fatigue Crack Growth Rate for Ferritic Steels in Light Water Reactor Environments," PVP–Vol. 286, Changing Priorities of Code and Standards, ASME, pp. 131–142, 1994.

23. Ford, F. P., Ranganath, S., and Weinstein, D., "Environmentally Assisted Fatigue Crack Initiation in Low–Alloy Steels – A Review of the Literature and the ASME Code Design Requirements," EPRI Report TR–102765, Aug. 1993.